

## Application of Al-decorated ZnO Nanorods as Gas Sensor to Detect H<sub>2</sub> and CO

Wei Chien,<sup>1,2</sup> Jang-Cheng Jheng,<sup>3</sup> Fang-Hsing Wang,<sup>3\*</sup> and Cheng-Fu Yang<sup>4,5\*\*</sup>

<sup>1</sup>Guangxi Key Laboratory of Ocean Engineering Equipment and Technology,  
12 Binhai Avenue, Qinzhou 535011, P.R. China

<sup>2</sup>Key Laboratory of Beibu Gulf Offshore Engineering Equipment and Technology (Beibu Gulf University),  
Education Department of Guangxi Zhuang Autonomous Region, 12 Binhai Avenue, Qinzhou 535011, P.R. China

<sup>3</sup>Graduate Institute of Optoelectronic Engineering, National Chung Hsing University,  
145 Xingda Rd., South Dist., Taichung City 40227, Taiwan

<sup>4</sup>Department of Chemical and Materials Engineering, National University of Kaohsiung,  
700, Kaohsiung University Rd., Nanzih District, Kaohsiung 811, Taiwan

<sup>5</sup>Department of Aeronautical Engineering, Chaoyang University of Technology,  
168, Jifeng E. Rd., Wufeng District, Taichung, 413310 Taiwan

(Received April 17, 2023; accepted July 31, 2023)

**Keywords:** Al-decorated ZnO, nanoarrays, gas sensor, hydrothermal method

In this paper, the synthesis of ZnO nanorods on a glass substrate using a hydrothermal method is described. First, spin coating was used to prepare a ZnO seed layer on a glass substrate. Then, hydrothermal synthesis was performed using a 0.03 M solution of Zn(CH<sub>3</sub>COO)<sub>2</sub>·2H<sub>2</sub>O, CH<sub>3</sub>OCH<sub>2</sub>CH<sub>2</sub>OH, and C<sub>2</sub>H<sub>7</sub>N and different synthesis times (30, 45, and 60 min) to synthesize ZnO nanorods on the ZnO seed layer. To improve the detection efficiency of both H<sub>2</sub> and CO, a 5-nm-thick aluminum layer was deposited on the surfaces of the synthesized ZnO nanorods by thermal evaporation. To create a metal–semiconductor–metal gas sensor, 350-nm-thick interdigitated aluminum electrodes were deposited on the ZnO nanorods. The thus-obtained sensor was used to measure the concentrations of H<sub>2</sub> and CO at temperatures ranging from 50 to 300 °C and at concentrations ranging from 100 to 2000 ppm. We compared the measurement results for pure and Al-decorated ZnO nanorods to determine the optimum sensing parameters. The measurement results showed the enhancements of the sensing efficiencies of H<sub>2</sub> and CO when Al was used to decorate ZnO nanorods.

### 1. Introduction

Zinc oxide (ZnO) can be used as a gas sensor, because the oxygen adsorbed on its surface reacts with specific gases, resulting in charge transfer, which changes its resistance. One-dimensional nanostructures, such as ZnO nanorods (or nanowires), possess a larger surface area to volume ratio than typical bulk material structures, making them suitable for gas-sensing applications.<sup>(1)</sup> Increasing the surface area to volume ratio of ZnO nanorods can improve the resistance response and the reaction time to the sensing gas. A larger surface area can greatly

\*Corresponding author: e-mail: [ansen@dragon.nchu.edu.tw](mailto:ansen@dragon.nchu.edu.tw)

\*\*Corresponding author: e-mail: [cfyang@nuk.edu.tw](mailto:cfyang@nuk.edu.tw)

<https://doi.org/10.18494/SAM4458>

increase the ratio of the surface energy of ZnO nanorods to the total energy, thereby improving the physical and chemical properties of ZnO nanorods compared with those of bulk materials. The hydrothermal method is the preferred technique for growing ZnO nanorods because of its low reaction temperature (typically below 100 °C)<sup>(2,3)</sup> and the ability to facilitate growth on an unpatterned<sup>(4,5)</sup> or patterned substrate.<sup>(6,7)</sup> External conditions such as temperature, supersaturation, and pH in the aqueous environment, in addition to the composition of the internal structure, can also affect the growth characteristics of ZnO nanorods.<sup>(4,8)</sup> In the applications of ZnO nanorods, their size and the spacing between them affect the device characteristics. To apply ZnO nanorods with different sizes and spacings to gas sensors, selective-area growth has become increasingly important. The technology employed for the selective-area growth of nanorod structures has undergone optimization, resulting in a move from micron or submicron features to nanosize features as device sizes have decreased and densities have increased. Moreover, the addition of precious or decorated metals on the surfaces of ZnO nanorods has increased the response and reduced the response time of traditional ZnO nanorod gas sensors, thus accelerating the changes in their electrical properties.<sup>(9,10)</sup>

Carbon monoxide (CO) due to incomplete combustion from water heaters and gas stoves has long been a serious concern for home safety as it can lead to CO poisoning. In addition, hydrogen (H<sub>2</sub>) is commonly used in industrial applications and is flammable, with concentrations above 4% in the atmosphere posing a risk of explosion. Therefore, CO and H<sub>2</sub> were chosen as the target gases for this study. However, the reaction and recovery rates are enhanced, leading to the preparation of a gas sensor with high safety. Unpatterned ZnO nanorods were grown on a glass substrate and decorated with Al metal nanoparticles for gas sensing. These nanoparticles can act as catalysts in the metal–oxide–semiconductor structure to further enhance the surface chemical heterogeneity, thereby improving the sensor response.<sup>(11)</sup> In this study, the hydrothermal method was employed to synthesize ZnO nanorods on a glass substrate. The resulting Al-decorated ZnO nanorods were used as sensors for detecting H<sub>2</sub> and CO. Measurements were conducted at different gas concentrations ranging from 100 to 2000 ppm and at temperatures ranging from 50 to 300 °C to determine the optimal operating conditions for gas detection. When the measurement results of ZnO nanorod sensors without and with Al decoration were compared, we found the enhancements of the sensing efficiencies of H<sub>2</sub> and CO when Al was used to decorate ZnO nanorods.

## 2. Experimental Procedure

In this study, a ZnO seed layer was grown on a Corning Eagle XG glass substrate, which was followed by the growth of ZnO nanorods by the hydrothermal method without patterning. The steps are illustrated in Fig. 1. First, the substrate was cleaned and used as a base to deposit a ZnO seed layer [step (a)]. Then, a ZnO gel was spin-coated on the substrate at a rotation speed of 2,000 rpm for 30 s. The coated ZnO film was then annealed at 300 °C for 10 min to volatilize the organic solvent and harden the coating film. The spin coating and baking processes were repeated six times [step (b)]. After that, ZnO nanorods were synthesized using a 0.03 M solution of Zn(CH<sub>3</sub>COO)<sub>2</sub>·2H<sub>2</sub>O, CH<sub>3</sub>OCH<sub>2</sub>CH<sub>2</sub>OH, and C<sub>2</sub>H<sub>7</sub>NO at 90 °C for different synthesis times

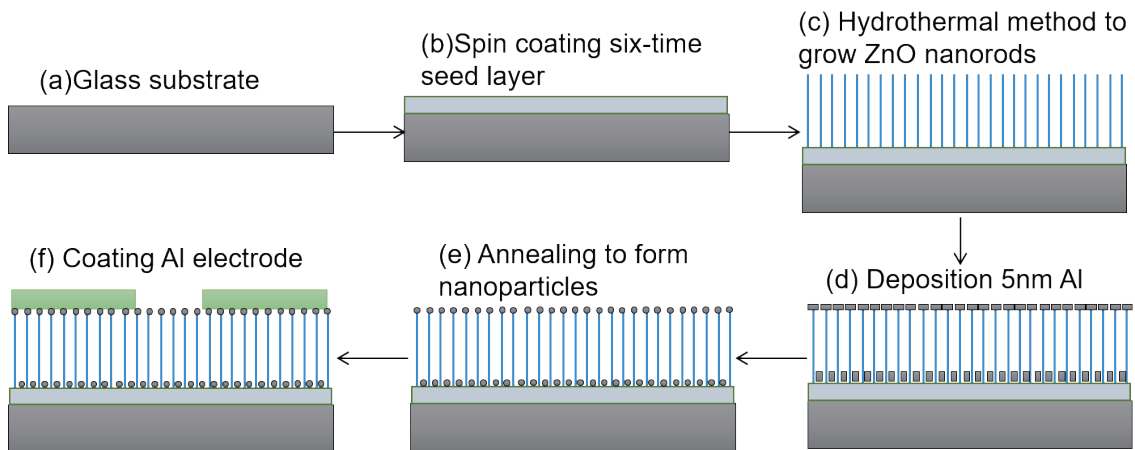


Fig. 1. (Color online) Schematic of fabrication of Al-decorated ZnO nanorod gas sensor.

[30, 45, and 60 min; step (c)]. Subsequently a 5-nm-thick aluminum film was deposited on the ZnO nanorods by thermal evaporation [step (d)]. Then, the samples were annealed at 550 °C for 10 min to convert the deposited Al film into nanoparticles [NPs; step (e)]. Finally, an interdigitated aluminum film was deposited by thermal evaporation, completing the fabrication of the sensor [step (f)].

After synthesizing the ZnO nanorods on the ZnO seed layer, we analyzed their crystalline phases by measuring their X-ray diffraction spectra. We also observed the surface morphologies of the nanorods using field-emission scanning electron microscopy. To observe cross-sectional morphologies, we cut the prepared ZnO seed layer and ZnO nanorods using a focused ion beam system. The photoluminescence (PL) properties of the nanorods were measured using a Hitachi F-4500 fluorescence spectrophotometer at room temperature, with measurements taken in the range of 350–650 nm. Following the deposition of Al electrodes on the ZnO nanorods, the devices were subjected to pretreatment at 350 °C for 1 h while passing air through the measurement chamber. A Keithley 2400 source meter was used to supply voltage and record the measured data via a computer connection. The chamber was pumped to  $10^{-2}$  Torr, and the stage within the cavity was heated directly to 400 °C. Table 1 presents different parameters of the gas used in the measurements.

### 3. Results and Discussion

The surface and cross-sectional morphologies of the ZnO nanorods grown with different synthesis times are compared in Figs. 2 and 3, respectively. The two figures show that the average diameter and length of the ZnO nanorods increased with the synthesis time. For the synthesis times of 30, 45, and 60 min, the average diameters were 68 nm (the largest and smallest diameters were 72 and 63 nm), 85 nm (89 and 82 nm), and 96 nm (100 and 91 nm), as shown in Fig. 2, and the average lengths of the ZnO nanorods were 778 nm (the longest and shortest lengths were 802 and 751 nm), 1005 nm (1033 and 978 nm), and 1018 nm (1046 and 992 nm), as

Table 1  
Concentrations and other parameters of the measured gas.

Preset concentration (ppm)	Inlet gas flow (sccm)	Inlet gas time (s)
100	50	5
500	200	6.25
1000	200	12.5
1500	200	18.75
2000	200	25

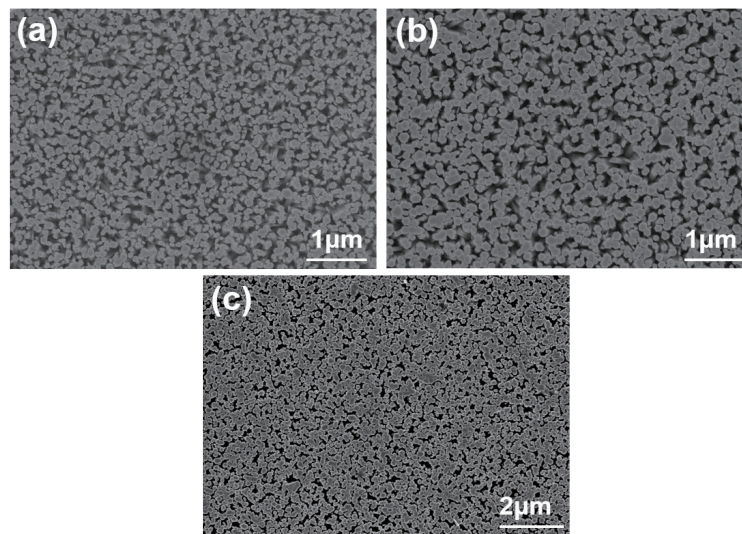


Fig. 2. Surface morphologies of ZnO nanorods with synthesis times of (a) 30, (b) 45, and (c) 60 min.

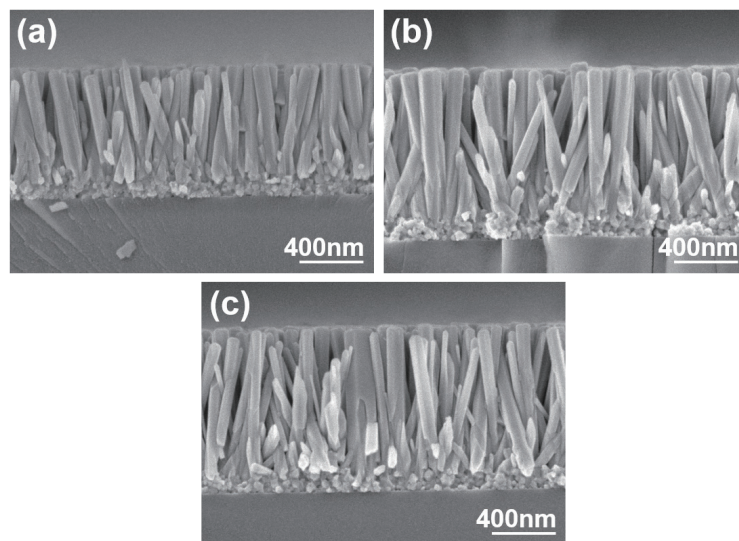


Fig. 3. Cross-sectional morphologies of ZnO nanorods with synthesis times of (a) 30, (b) 45, and (c) 60 min.

shown in Fig. 3, respectively. Furthermore, controlling parameters such as the growth time and solution concentration in the hydrothermal method can cause the fusion of the nanorods. Li *et al.* investigated the mechanism of fused growth in ZnO columns and found that ZnO columns with large diameters were obtained from the fused growth of fine ZnO columns with small diameters.<sup>(12)</sup> During the initial growth stage, the bottom parts of the nanorods came in contact with each other, causing the entire bundle of fine ZnO nanorods to fuse into a larger hexagonal ZnO nanorod. This was due to fine ZnO nanorods having a lower surface energy than wide nanorods during the synthesis of the ZnO nanorods. The average lengths of the ZnO nanorods grown with synthesis times of 45 and 60 min were very similar. The obtained result serves as evidence for the underlying mechanism, which can be attributed to the varying thickness of each seed layer. Specifically, the thickness of each seed layer falls within the range of 19 to 31 nm, with a notable variation of 12 nm across individual layers.

During the synthesis, two adjacent nanorods combined to form a single nanorod, resulting in an increase in nanorod diameter and a decrease in nanorod density. The nanorod density was calculated by selecting five points from the top, bottom, left, right, and middle of the SEM images. A square with an area of  $1 \mu\text{m}^2$  was then drawn around each of the five points, and the number of ZnO nanorods in each square was counted, then the five values were averaged.<sup>(6,7)</sup> For the synthesis times of 30, 45, and 60 min and finding the average results measured in five squares, the average number and total surface area of the ZnO nanorods in a  $1 \mu\text{m}^2$  square were determined to be 149, 105, and 95, and 12.01, 18.77, and  $23.94 \mu\text{m}^2$ , respectively. These values also increase with the synthesis time, with the 60-min-synthesized ZnO nanorods having the largest surface area. Therefore, we used the 60-min-synthesized ZnO nanorods as a device for gas sensors in this study. The average areas of the top areas of the synthesized ZnO nanorods in each square are 0.15, 0.47, and  $0.60 \mu\text{m}^2$  for synthesis times of 30, 45, and 60 min, respectively. Consequently, the average volumes of the ZnO nanorods in each square are 0.81, 1.6, and  $2.3 \mu\text{m}^3$ , respectively, which also increase with synthesis time. Table 2 provides a summary of the properties of the ZnO nanorods synthesized for different times.

All the ZnO nanorods synthesized for different times exhibited similar X-ray diffraction (XRD) patterns, and the XRD pattern of the ZnO nanorods synthesized for 45 min is presented in Fig. 4. A comparison with the JCPDS database revealed that the diffraction peaks correspond to the wurtzite structure of ZnO. The intensity of the diffraction peak in the (002) direction at around  $34.6^\circ$  is considerably higher than those of the other peaks, indicating that the ZnO nanorods are preferentially oriented in the c-axis direction, resulting in a stress value close to

Table 2  
Comparison of properties of ZnO nanorods synthesized on glass substrates as a function of synthesis time.

Synthesis time (min)	30	45	60
Diameter ( $D$ , nm)	68	85	96
Length ( $L$ , nm)	778	1005	1018
Aspect ratio ( $L/D$ )	11.4	11.8	10.6
Density ( $\mu\text{m}^{-2}$ )	149	105	95
Total surface area ( $\mu\text{m}^2$ )	12.01	18.77	23.94
Total top surface area ( $\mu\text{m}^2$ )	0.15	0.47	0.60
Average volume ( $\mu\text{m}^3$ )	0.81	1.6	2.3

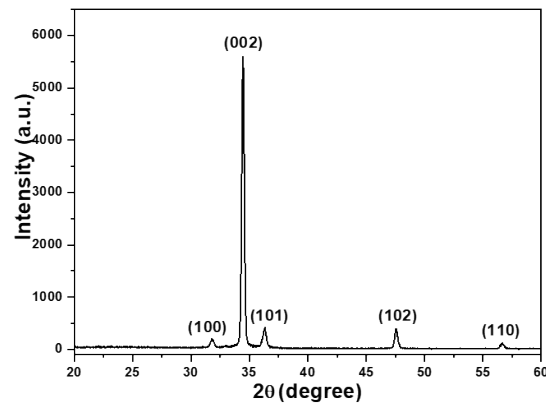


Fig. 4. XRD pattern of 45-min-synthesized ZnO nanorods.

zero. From the full width at half maximum of the (002) diffraction peak and the Debye–Scherrer equation, the particle size of the ZnO nanorods was calculated to be 31.99 nm.

Figure 5(a) provides a visual representation of the specific range of analysis conducted during the energy-dispersive X-ray spectroscopy (EDS) analysis of the ZnO nanorods grown on glass substrates decorated with Al. The growth time for the ZnO nanorods was 60 min, as mentioned earlier. To verify Al deposition on the ZnO nanorods, the backscattered electrons obtained by SEM were utilized. The results of this analysis are depicted in Fig. 5(b). The obtained data clearly indicate the detection of both Al and Zn on the nanorod surfaces. Additionally, the presence of Ca was observed. It is important to note that the analysis was conducted from top to bottom, which suggests that the detected Ca most likely originated from the glass substrate rather than the ZnO nanorods themselves. This information provides valuable insights into the composition and structure of the ZnO nanorods and the effectiveness of the Al decoration on the glass substrates.

The ZnO nanorods synthesized in the study had different defect densities, and the PL spectrum is an important tool for comparing the defects of ZnO nanorods. Figure 6(a) shows the PL spectra of the ZnO nanorods synthesized for different times and excited at a wavelength of 325 nm. The nanorods exhibited two emission peaks, namely, the UV emission peak at approximately 380 nm and the visible green emission peak at approximately 450 to 550 nm. The UV emission peak results from the recombination of free excitons (free excitons) of the ZnO itself, which is also known as the near-band edge emission. The green (495–570 nm) and yellow (570–590 nm) emission peaks arise from the recombination of conduction band electrons with deeper-level holes. The green emission peak is caused by oxygen vacancies, whereas the yellow (or orange, at 590–620 nm) emission peak is caused by interstitial oxygen ions. Figure 6(a) also shows that the UV and green emission peak intensities increase with the growth time. The increase in green emission peak intensity suggests an increase in the defect density of ZnO nanorods with the synthesis time. The increase in UV emission peak intensity is primarily due to the increased length and diameter of the ZnO nanorods with the synthesis time, resulting in increases in the surface area of the tops and the total volume, and, consequently, an increase in

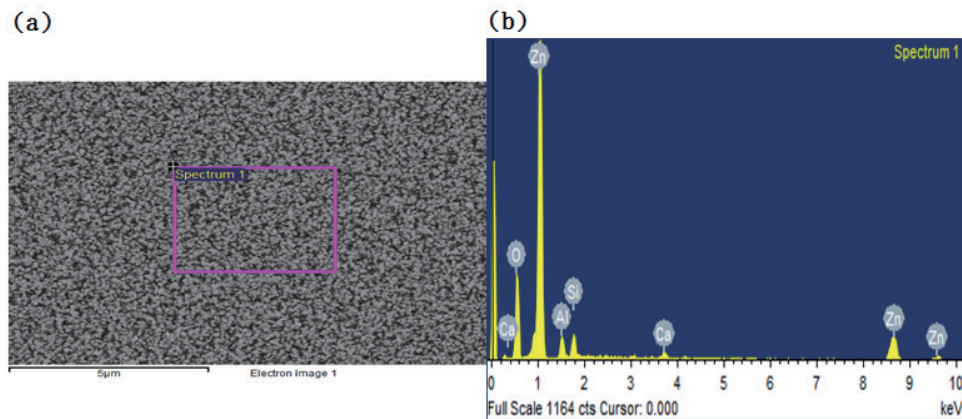


Fig. 5. (Color online) EDS analysis of grown ZnO nanorods decorated with Al: (a) selection range and (b) elements' peak.

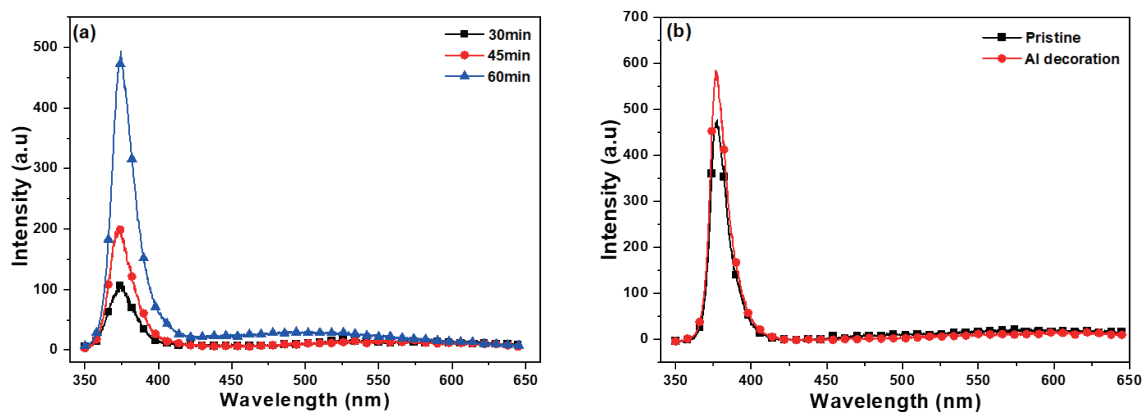


Fig. 6. (Color online) PL spectra of (a) ZnO nanorods with different synthesis times and (b) 60-min-synthesized ZnO nanorods without and with Al decoration.

UV emission peak intensity. Figure 6(b) displays the PL spectra of the ZnO nanorods synthesized for 60 min with and without Al decoration. The figure indicates that the UV emission intensity of the Al-decorated ZnO nanorods was higher than that of the undecorated ones. These findings imply that Al decoration alters the PL characteristics of ZnO nanorods, consequently affecting the sensing capabilities of the nanorods towards  $H_2$  and CO gases.

When conducting measurements with varying temperature, we observed changes in resistance and resistance response by introducing  $H_2$  and CO gases at 2000 ppm, as well as air. The comparison of these results can be seen in Fig. 7(a). The resistances of the pristine and Al-decorated ZnO nanorods were measured in air and at temperatures of 50 °C (300 °C), yielding values of 213.6 and 211.7 k $\Omega$  (50.1 and 49.3 k $\Omega$ ), respectively. Interestingly, when  $H_2$  and CO gases were introduced, the resistance of pristine ZnO nanorods at 50 °C remained relatively unchanged. In contrast, the resistance of Al-decorated ZnO nanorods decreased significantly to 170 k $\Omega$ . This notable reduction indicates that Al can act as a catalyst, enhancing the responses of the nanorods to  $H_2$  and CO gases.

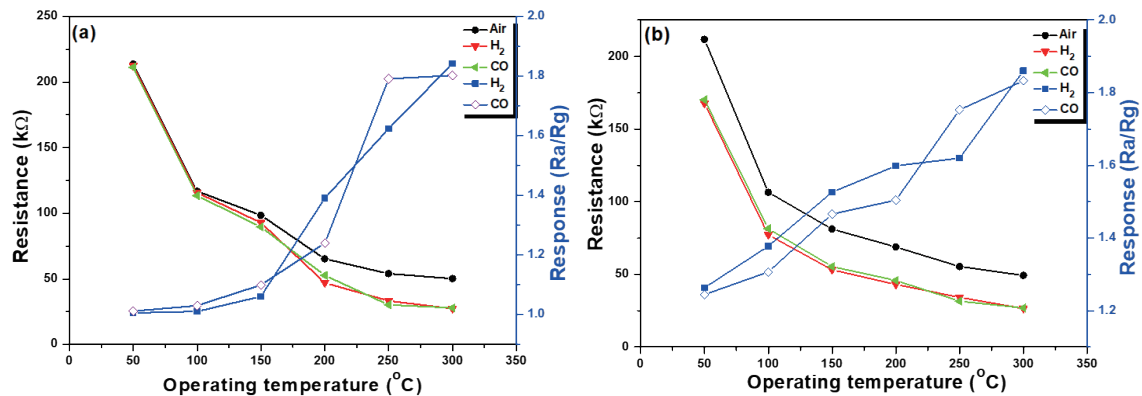


Fig. 7. (Color online) Temperature-dependent resistance and response of gas sensors for different gases at 2000 ppm: (a) pristine and (b) Al-decorated ZnO nanorods.

Figure 7(b) demonstrates that the differences in resistance between the Al-decorated ZnO nanorods at 50 and 300 °C remain similar when H<sub>2</sub> and CO gases are introduced. This finding further indicates that Al-decorated ZnO nanorods exhibit stable catalytic characteristics even at temperatures of up to 300 °C. Moreover, Fig. 7(b) reveals that the response of pristine ZnO nanorods slightly increases with the temperature up to 200 °C but markedly increases above 200 °C. In contrast, the response ratio of the Al-decorated ZnO nanorods increases linearly with the measurement temperature from 50 to 300 °C. These results demonstrate that the Al-decorated ZnO nanorods exhibit superior sensing properties for H<sub>2</sub> and CO gases to the pristine ZnO nanorods.

#### 4. Conclusions

ZnO nanorods were successfully synthesized on a glass substrate and their growth properties were thoroughly investigated. For synthesis times of 30, 45, and 60 min, the average lengths of the ZnO nanorods were 778, 1005, and 1018 nm and the average diameters were 68, 85, and 96 nm, respectively. In a 1 μm<sup>2</sup> square, the average numbers of nanorods were 149, 105, and 95, the total surface areas were 12.01, 18.77, and 23.94 μm<sup>2</sup>, and the volumes were 0.81, 1.6, and 2.3 μm<sup>3</sup>, respectively. The maximum and minimum sizes of Al nanoparticles were 41.67 and 25 nm, respectively. Both undecorated and Al-decorated ZnO nanorods were fabricated as sensors of H<sub>2</sub> and CO. The resistances of the Al-decorated ZnO nanorods were significantly lower in H<sub>2</sub> and CO than in air. Moreover, their response ratio increased linearly with the measurement temperature from 50 to 300 °C. These findings indicate that Al-decorated ZnO nanorods have higher H<sub>2</sub> and CO sensing properties than pristine ZnO nanorods.

#### Acknowledgments

This work was supported by the projects under Nos. MOST 110-2622-E-390-002, MOST 110-2221-E-390-020, and MOST 111-2221-E-390-018.



## References

- 1 D. Barreca, D. Bekermann, E. Comini, A. Devi, R. A. Fischer, A. Gasparotto, C. Maccato, G. Sberveglieri, and E. Tondello: *Sens. Actuators, B* **149** (2010) 1.
- 2 S. Worasawat, T. Masuzawa, Y. Hatanaka, Y. Neo, H. Mimura, and W. Pecharapa: *Mater. Today: Proc.* **5** (2018) 10964.
- 3 K. Edalati, A. Shakiba, J. Vahdati-Khaki, and S. M. Zebarjad: *Mater. Res. Bull.* **74** (2016) 374.
- 4 Y. F. Wei, W. Y. Chung, C. F. Yang, W. F. Hsu, and C. C. Chen: *Sens. Mater.* **31** (2019) 3619.
- 5 K. Ahmadi, A. A. Ziabari, K. Mirabbaszadeh, and A. A. Shal: *Bull. Mater. Sci.* **38** (2015) 617.
- 6 C. F. Yang, C. S. Wang, F. H. Wang, H. W. Liu, and J. Micova: *Appl. Funct. Mater.* **2** (2022) 44.
- 7 C. Y. Lee, C. S. Wang, F. H. Wang, H. W. Liu, and C. F. Yang: *ACS Omega* **7** (2022) 17384.
- 8 Y. C. Chen, H. Y. Cheng, C. F. Yang, and Y. T. Hsieh: *J. Nanomater.* **2014** (2014) 430164.
- 9 C. V. V. M. Gopi, M. Venkata-Haritha, Y. S. Lee, and H. J. Kim: *J. Mater. Chem. A* **4** (2016) 8161.
- 10 S. K. Mandal, S. Paul, S. Datta, and D. Jana: *Appl. Sur. Sci.* **563** (2021) 150315.
- 11 Y. C. Wang, I. C. Leu, and M. H. Hon: *Electrochem. Solid-State Lett.* **5** (2002) C53.
- 12 Q. Li, V. Kumar, Y. Li, H. Zhang, T. J. Marks, and R. P. H. Chang: *Chem. Mater.* **17** (2005) 1001.